Testing for a CO_2 fertilization effect on growth of Canadian boreal forests

Martin P. Girardin[1], Pierre Y. Bernier[1], Frédéric Raulier[2], Jacques C. Tardif[3], France Conciatori[3], Xiao Jing Guo[1]

1. Natural Resources Canada, Canadian Forest Service, Laurentian Forestry Centre, 1055 du P.E.P.S, P.O. Box 10380, Stn. Sainte-Foy, Quebec, QC, G1V 4C7, Canada
2. Faculté de foresterie et de géomatique, Université Laval, Quebec, QC, G1K 7P4, Canada.
3. Canada Research Chair in Dendrochronology, Centre for Forest Interdisciplinary Research (C-FIR), University of Winnipeg, 515 Portage Avenue, Winnipeg, MB, R3B 2E9, Canada

Under publication in Journal of Geophysical Research - Biogeosciences
2010JG001287RR

Corresponding author:
Martin P. Girardin
Natural Resources Canada
Canadian Forest Service
Laurentian Forestry Centre
1055 du P.E.P.S.
P.O. Box 10380
Stn. Sainte-Foy
Quebec, Quebec
G1V 4C7
Canada
Tel: (418) 648-5826
Fax: (418) 648-5849
E-mail: Martin.Girardin@rncan.gc.ca

Abstract

The CO_2 fertilization hypothesis stipulates that rising atmospheric CO_2 has a direct positive effect on net primary productivity (NPP), with experimental evidence suggesting a 23% growth enhancement with a doubling of CO_2. Here, we test this hypothesis by comparing a bioclimatic model simulation of NPP over the 20th century against tree growth increment (TGI) data of 192 *Pinus banksiana* trees from the Duck Mountain Provincial Forest in Manitoba, Canada. We postulate that, if a CO_2 fertilization effect has occurred, climatically driven simulations of NPP and TGI will diverge with increasing CO_2. We use a two-level scaling approach to simulate NPP. A leaf-level model is first used to simulate high-frequency responses to climate variability. A canopy-level model of NPP is then adjusted to the aggregated leaf-level results and used to simulate yearly plot-level NPP. Neither model accounts for CO_2 fertilization. The climatically driven simulations of NPP for 1912–2000 are effective for tracking the measured year-to-year variations in TGI, with 47.2% of the variance in TGI reproduced by the simulation. In addition, the simulation reproduces without divergence the positive linear trend detected in TGI over the same period. Our results therefore do not support the attribution of a portion of the historical linear trend in TGI to CO_2 fertilization at the level suggested by current experimental evidence. A sensitivity analysis done by adding an expected CO_2 fertilization effect to simulations suggests that the detection limit of the study is for a 14% growth increment with a doubling of atmospheric CO_2 concentration.

Key words CO_2 enhancement, dendrochronology, process-based model, boreal forest, jack pine

1. Introduction

The CO_2 fertilization hypothesis stipulates that rising atmospheric CO_2 has a positive effect on net primary productivity (NPP) due to increasing availability of carbon, a limiting factor for the photosynthesis of C_3 plants [*Huang et al.*, 2007]. The concept of CO_2 fertilization has a long experimental history and has been well demonstrated under laboratory or controlled conditions for a variety of C_3 vascular plants, including trees [see reviews by *Norby et al.*, 1999; *Ainsworth and Long*, 2005; *Huang et al.*, 2007; *Körner et al.*, 2007; *Wang*, 2007; *Prentice and Harrison*, 2009]. In a landmark paper, *Norby et al.* [2005] have reported on the most extensive experiments on this topic involving multi-year free-air CO_2 enrichment (FACE) in coniferous and deciduous plantations. In the four sites under study, they have found a 23% enhancement of NPP sustained over multiple years following a doubling of pre-industrial CO_2 concentrations. Given the current weight of experimental evidence, modellers have been including CO_2 fertilization effects in their simulations of past and future forest productivity [e.g. *Rathgeber et al.*, 2000, 2003; *Chen et al.*, 2000; *Balshi et al.*, 2007; *Su et al.*, 2007; *Peng et al.*, 2009], generally resulting in projected increases in forest growth under future atmospheric CO_2 concentrations. The impact of this type of inclusion is important as predictions of forest carbon sequestration dynamics are increasingly coupled to global circulation models and CO_2 emission scenarios [e.g. *Notaro et al.*, 2007; *O'ishi et al.*, 2009].

In spite of the current wealth of experimental evidence on CO_2 fertilization of tree growth, there is still some doubt as to the actual realization of this effect under natural conditions. *Körner et al.* [2005], in a FACE experiment in a mature deciduous forest, have found no lasting growth stimulation by CO_2 enrichment after 4 years of treatment.

Caspersen et al. [2000], in a study of long-term results from forest sample plots in the eastern United States, have found only a modest increase in tree growth over the past century. And recently, *Norby et al.* [2008, 2009] reported that nitrogen limitation was causing a dramatic reduction in growth enhancement in their hardwood FACE experiment from the 23% reported in *Norby et al.* [2005] to a current value of 9%. Evidences of site fertility restrain on carbon sequestration were also found by Oren *et al.* [2001] in their study of mature pine forests exposed to elevated atmospheric CO_2. In their global simulations of CO_2-enhancement on NPP, *Hickler et al.* [2008] concluded that current FACE results do not apply to boreal forest, because of the strong temperature dependence of the relative affinity of the carboxylation enzyme Rubisco for CO_2 and O_2. The predominantly colder temperatures of boreal forests compared with FACE experiments would limit the CO_2 effect, with a simulated increased of NPP of about 15% under a doubling of atmospheric CO_2 [*Hickler et al.*, 2008]. These reports raise the question of the importance of CO_2 fertilization in natural forest environments where tree growth is limited by other factors.

As mentioned above, CO_2 fertilization effects on growth have already been included in many process-based models. Such models serve as direct links between the climate and tree growth [*Hunt et al.*, 1991; *Landsberg and Waring*, 1997; *Rathgeber et al.*, 2000; 2003; *Misson et al.*, 2004] or ecosystem carbon dynamics [e.g. *Balshi et al.*, 2007; *Peng et al.*, 2009]. The challenge with any such inclusion, however, lies with the verification of the modeled change in growth against actual field measurements of realized growth. Because real-world CO_2 enhancement is not a step function, but rather a long-term monotonic increase, the signal it generates in tree growth is not easily

99 detectable. The signal is certainly far weaker than the large inter-annual variations caused
100 by climate variability [*D'Arrigo and Jacoby*, 1993] and may be within the uncertainties
101 related to forest inventory data [*Joos et al.*, 2002]. In addition, global temperatures have
102 also been increasing, along with atmospheric nitrogen deposition in some parts of the
103 globe, further confounding the effect of CO_2 fertilization. Finally, the response of plants
104 to CO_2 is also affected by the possible down-regulation of photosynthesis [e.g. *Eguchi*,
105 2008; *Crous et al.,* 2008]. All these issues make the detection of CO_2 fertilization effects
106 particularly challenging.

107 Here, we test the CO_2 fertilization hypothesis by comparing tree growth increment
108 data from 1912 to 2000 with simulation results using a simulator that does not
109 incorporate CO_2 fertilization effects, and is empirically adjusted to the current CO_2
110 growth environment through field measurements of photosynthesis. We postulate that, in
111 the event that a CO_2 fertilization effect has occurred, climatically driven simulations of
112 forest productivity will show increasing divergence with the measurement record over
113 time as the atmospheric CO_2 increases [*Graumlich*, 1991; *Jacoby and D'Arrigo*, 1989;
114 1997; *Rathgeber et al.*, 2000]. For this purpose, we used tree-ring increments of 192 jack
115 pine (*Pinus banksiana* Lamb.) trees from the closed-canopy boreal forest of Duck
116 Mountain Provincial Forest (DMPF) in Manitoba, Canada. Growth increment data were
117 transformed into a tree growth index (TGI) using the regional curve standardization
118 technique, such that low-frequency signals were retained in the data. The final tree-ring
119 chronology extends from 1717 to 2000. We used a two-level scaling approach to achieve
120 estimates of forest productivity for the period of 1912 to 2000. At the finest scale, a leaf-
121 level model of photosynthesis (FineLEAP) was used to simulate canopy properties and

122 their interaction with the variability in radiation, temperature and vapour pressure deficit.
123 Then, the StandLEAP model, a top-down plot-level model of forest productivity, was
124 used to simulate landscape-level productivity over the 20th century. The two levels of
125 simulation are linked functionally as parameters of the coarser models are estimated from
126 aggregated simulation results of the finer model, but neither model accounts for CO_2
127 fertilization. Finally, the detection limit of our approach was investigated through a
128 sensitivity analysis in which an expected CO_2 fertilization was included in StandLEAP
129 simulations via a response function.
130

131 2. Study area

132 The study took place in the DMPF (51°40′N; 100°55′W), which covers approximately
133 376,000 ha (Fig. 1). Duck Mountain is located within the Boreal Plains ecozone, a
134 transition zone between the boreal forest to the north and the aspen parkland and prairie
135 to the south, and is topographically part of the Manitoba Escarpment, which is
136 characterized by a higher elevation compared with the surrounding plains (300–400 m
137 above sea level, with highest point at 825 m). Pure to mixed deciduous and coniferous
138 stands, primarily composed of trembling aspen (*Populus tremuloides* Michx.) and white
139 spruce (*Picea glauca* [Moench] Voss), constitute about 80% of the DMPF. Stands
140 dominated by black spruce (*Picea mariana* [Mill.] BSP) and jack pine constitute about
141 14% and 6% of the area, respectively, and occur most commonly in the central, higher
142 elevation regions of the DMPF. The DMPF has a mid-boreal climate with predominantly
143 short, cool summers and cold winters. At lower elevation Swan River (52°03′N;
144 101°13′W, elevation: 346.6 m asl), mean monthly temperatures ranged from –18.2°C in

145 January to 18.1°C in July for the reference period of 1971–2000. Average total annual
146 precipitation was 530.3 mm, with most precipitation falling as rain between May and
147 September.
148

149 3. Data

150 3.1. Tree-ring measurements

151 During the summers of 2000 and 2001, the DMPF was surveyed with the objective of
152 reconstructing fire history [*Tardif*, 2004]. The DMPF was systematically divided into
153 UTM grids (10 x 10 km) and sites were sampled within each grid based on accessibility.
154 Detailed information on data collection is found in *Tardif* [2004]. For the current study,
155 we analysed a subset of jack pine cores (2 radii/tree) and stem cross-sections consisting
156 of 192 living and dead trees collected from 70 sampling sites located within 20 UTM
157 grids. Only trees with complete ring measurements from pith to the last year of growth
158 were included, which explains the lower sample replication compared to earlier studies
159 [i.e., 291 trees in that of *Girardin and Tardif*, 2005]. The majority of samples were
160 collected in the uplands in stands dominated by jack pine and black spruce. Each of the
161 cores and sections were dried, sanded and cross-dated using the pointer-year method
162 [*Yamaguchi*, 1991]. Annual growth increments were measured from the pith to the
163 outermost ring at a precision of 0.001 mm using a Velmex measuring stage coupled with
164 a computer, and both cross-dating and measurements were statistically validated using
165 the COFECHA program [*Holmes*, 1983]. The final dataset consisted of 332 ring-width

166 measurement series. Ring-width measurements were recorded for a period extending
167 from AD 1717 to AD 2000.
168

169 3.2 Meteorological data

170 Meteorological data used as input for the bioclimatic model were monthly means of daily
171 maximum and minimum temperatures (from the Birtle [1905–1998] and Dauphin
172 [1904–2003] meteorological stations; Fig. 1) and total monthly precipitation data (from
173 the Birtle [1918–2000], Dauphin [1912–2003], and Russell [1916–1990] meteorological
174 stations) from *Vincent and Gullett* [1999] and *Mekis and Hogg* [1999], respectively. Data
175 were corrected by the authors for non-homogeneities associated with changes in
176 instrumentation or weather station location. Regional climate data files were created by
177 averaging data from all stations following the procedure described in *Fritts* [1976]
178 (homogeneity testing, station adjustments for mean and standard deviation, and station
179 averaging).
180

181 3.3 Forest inventories

182 Biometric information was obtained from DMPF temporary sample plots (TSP) of the
183 Forest Lands Inventory initiated by Louisiana Pacific Canada Ltd.–Forest Resources
184 Division and Manitoba Conservation–Forestry Branch. Necessary information for driving
185 the StandLEAP bioclimatic model includes soil texture and forest stand properties (forest
186 composition and biomass estimates). For simplicity, we only modelled forest stands
187 classified as “pure” jack pine stands (i.e., where more than 75% of plot basal area was

188 contributed by jack pine). A total of ten plots (out of 1317) met the 75% criterion while
189 also having all the necessary information for modelling purposes (auxiliary material
190 Table S1). For each of these TSPs, aboveground biomass was estimated using the
191 national biomass equations of *Lambert et al.* [2005]. These functions were applied to
192 each tree, and the individual tree biomass values were summed to estimate stand-level
193 biomass density (Mg ha^{-1}) in each TSP.
194

195 3.4 Atmospheric CO_2 data

196 We used annual average of the atmospheric concentrations of CO_2 reconstructed from ice
197 cores [*Etheridge et al.*, 1996] and recorded at Mauna Loa observatory since 1953
198 [*Keeling et al.*, 1982]. The CO_2 concentration increased from 300 ppmv in 1910, to 317
199 ppmv in 1960, and to 370 ppmv in 2000.
200

201 4. Methods

202 4.1 Development of the tree growth index (TGI)

203 All ring-width measurements were detrended using the regional curve standardization
204 technique [*Esper et al.*, 2003] in order to eliminate noise caused by site-related effects
205 (e.g. competition and self-thinning) and biological effects (e.g. aging). This approach has
206 the potential to preserve the evidence of long time scale forcing of tree growth [see
207 reviews by *Esper et al.*, 2003 and *Briffa and Melvin*, in press] as it scales ring-width
208 measurements against an expectation of growth for the appropriate age of each ring (Fig.

209 2). We first aligned the 332 measurement series by cambial age and calculated the
210 arithmetic mean of ring width for each ring age. We then created a regional curve (RC)
211 by applying a negative exponential smoothing [*Cook and Kairiukstis*, 1990] to the age
212 series of arithmetic means (Fig. 2). It is assumed that this RC created from the means of
213 ring width for each ring age describes the functional form of the age-related growth trend.
214 Note that our conclusions were insensitive to the use of other types of smoothing [e.g. the
215 'Hugershoff' or spline smoothing; *Cook and Kairiukstis*, 1990] or to truncation of the
216 measurement series by removal of the juvenile period (first 15 to 20 years of data) and
217 downsampling of age cohorts (auxiliary material Figs. S1, S2 and S3). Next, we divided
218 each one of the original 332 ring-width measurement series by the RC value for the
219 appropriate ring age to create standardized series. These departures from the RC are
220 interpreted as departures related to climate variability or some other induced forcing (e.g.
221 insect herbivory). Finally, the 332 standardized series were realigned by calendar year
222 and averaged using a bi-weight robust mean to create the jack pine tree growth index
223 (TGI). TGI error was estimated by bootstrapping the standardized series and collecting
224 the two-tailed 95% confidence interval from the distribution of the bootstrapped means.
225 Robustness of the final jack pine chronology was assessed using a 30-year 'moving
226 window' approach of the inter-series correlation, and of the expressed population signal
227 (EPS) [*Wigley et al.*, 1984]. The EPS is a measure of the degree to which the mean
228 chronology represents the hypothetical perfect, noise-free, chronology. The EPS ranges
229 from zero to one. A value of 0.85 has been tentatively suggested as desirable [*Wigley et*
230 *al.*, 1984]. Program ARSTAN (version 40c) was used for processing of tree-ring
231 measurement series and for computation of statistics [*Cook and Krusic*, 2006].

4.2 Modelling of forest productivity

The bioclimatic model StandLEAP version 2.1 [*Raulier et al.*, 2000; *Girardin et al.*, 2008] was used to simulate past forest productivity. StandLEAP is based on the 3PG model [*Landsberg and Waring*, 1997], and is a generalized stand model applicable to even-aged, relatively homogeneous forests. It is parameterized for individual species. Application of StandLEAP to any particular stand does not involve the use of error reduction techniques. We conducted monthly simulations of forest productivity (described below) for each of the ten temporary sample plots of the DMPF Lands Inventory (auxiliary material Table S1). Monthly simulation outputs were summed to seasonal and annual values, and plots were averaged to a regional level. Sampling error was estimated by bootstrapping the simulations and collecting the two-tailed 95% confidence interval from the distribution of the bootstrapped means.

In StandLEAP, absorbed photosynthetically active radiation (APAR, mol m^{-2} $month^{-1}$) is related to gross primary productivity (GPP, gC m^{-2} $month^{-1}$) using a radiation use efficiency coefficient (RUE; gC/mol^{-1} APAR):

[eq. 1] $GPP = APAR \times RUE$,

where

[eq. 2] $RUE = \overline{RUE} \times f_1 f_2 ... f_n$.

255 $\overline{\mathrm{RUE}}$ represents a species-specific mean value of RUE. The value of RUE differs among
256 locations and through time because of the occurrence of environmental constraints on the
257 capacity of trees to use APAR to fix carbon. Each constraint takes on the form of a
258 species-specific multiplier ($f_1 \ldots f_n$) with a value usually close to unity under average
259 conditions, but which can decrease towards zero to represent increasing limitations (e.g.
260 soil water deficit), or increase above 1.0 as conditions improve towards optimum (e.g.
261 temperature). Constraints related to mean maximum and minimum daily soil and air
262 temperatures, vapour pressure deficit (VPD), monthly radiation, and leaf area index are
263 expressed using a quadratic function:
264
265 [eq. 3] $$f_x = 1 + \beta_{lx}\left(\frac{x-\bar{x}}{\bar{x}}\right) + \beta_{qx}\left(\frac{x-\bar{x}}{\bar{x}}\right)^2 .$$
266
267 where parameters β_{lx} and β_{qx} represent the linear and quadratic effects of the variable x on
268 RUE and $\bar{x}$ is the mean value of the variable over the period of calibration. The
269 multipliers ($f_1 \ldots f_n$) account for non-linearity in time and space that cannot be accounted
270 for by a constant value of RUE.
271 Parameter values of eq. 3 for the f_x multipliers are derived from prior finer-scale
272 simulation results of canopy-level GPP and transpiration carried out using FineLEAP, a
273 species-specific multi-layer hourly canopy gas exchange model [*Raulier et al.*, 2000;
274 *Bernier et al.*, 2001, 2002]. In FineLEAP, the representation of photosynthesis is based
275 on the equations of *Farquhar et al.* [1980] parameterized from leaf-level instantaneous
276 gas exchange measurements, including the sensitivity of shoot photosynthesis to PAR,

277 temperature and VPD, and the characterization of the shoot physiological and light-
278 capturing properties with shoot age and surrounding average diffuse and direct light
279 environment. Transpiration was computed using the energy balance approach of *Leuning*
280 *et al.* [1995]. Sixty leaf angular classes were considered (five for the zenith and 12 for the
281 azimuth).

282 The FineLEAP model simulates canopies aspatially as layers of foliage of equal
283 properties by using the frequency distribution of the leaf area by classes of shoot age.
284 This aspatial approach rests on the strong relationship between leaf area per unit mass,
285 and both the photosynthetic properties of the foliage and the average light climate
286 impinging upon it [*Bernier et al.*, 2001]. Ecophysiological and canopy structure data for
287 jack pine were drawn mostly from the 1994 to 1996 BOREAS [*Sellers et al.*, 1997]
288 datasets for northern and southern study areas in old jack pine stands (98°37'19"W,
289 55°55'41"N and 104°41'20"W, 53°54'58" respectively). These data are archived at the
290 ORNL-DAAC [*Newcomer et al.*, 2000]. FineLEAP simulations were repeated for each
291 climate sequence and for a range of leaf area indices (2 to 8 m^2/m^2). Hourly values of
292 transpiration, of GPP, and of environmental variables derived from or used in FineLEAP
293 simulations were then rolled up into a monthly dataset. This new synthetic dataset was
294 used to fit simultaneously eqs. 1 and 2, in which modifier variables were expressed as in
295 eq. 3. The fit was performed in an iterative procedure with the gradual inclusion of
296 modifier variables in a declining order of significance. Only variables that reduced the
297 residual mean square error by more than 5% were retained [*Raulier et al.*, 2000]. The
298 atmospheric CO_2 concentration was assumed to be constant at 350 ppmv.

299 Other basic climate influences on productivity are encapsulated in StandLEAP
300 within the following functions. The multipliers used to represent the effect of soil water
301 content (f_θ) is as in *Landsberg and Waring* [1997], and that of frost (f_F) is as in *Aber et al.*
302 [1995]; both are limited to a maximum of 1.0. Bud burst and growth resumption in spring
303 takes place after the accumulation of a certain heat sum above a specific base temperature
304 [*Hänninen*, 1990]. Monthly APAR is adjusted throughout the growing season for changes
305 in leaf area due to phenological development, as in the PnET model [*Aber and Federer*,
306 1992].

307 Computation of NPP and respiration fluxes by the StandLEAP model is done as
308 follows. NPP (gC m^{-2} $month^{-1}$) is computed monthly after partitioning respiration into
309 growth (R_g, a fixed proportion of GPP) and maintenance (R_m) quantities and subtracting
310 these from GPP:

311

312 [eq. 4] $NPP = GPP - (R_g + R_m)$.

313

314 R_m (gC m^{-2} $month^{-1}$) is computed as a function of temperature using a Q_{10} relationship
315 [*Agren and Axelsson*, 1980; *Ryan*, 1991; *Lavigne and Ryan*, 1997]:

316

317 [eq. 5] $R_m = \sum (M \cdot r_{m10} Q_{10rm}^{(T_m - 10)/10})$

318

319 where M is the living biomass of each plant component and r_{m10} is their respective
320 respiration rate per gN at 10°C and Q_{10rm} is the temperature sensitivity of R_m, defined as
321 the relative increase in respiration for a 10°C increase in temperature. This function is

322 derived from the strong correlation between tissue nitrogen concentrations and plant
323 maintenance respiration [*Ryan*, 1991]. R_m is calculated separately for stem sapwood, root
324 sapwood, fine roots, and foliage. Similarly, net ecosystem productivity (NEP) is obtained
325 from
326
327 [eq. 6] $NEP = NPP - R_h$
328
329 where heterotrophic respiration (R_h) (gC m^{-2} $month^{-1}$) is computed as
330
331 [eq. 7] $R_h = y_0 + ae^{bT}$
332
333 where T represents monthly mean temperature. Values of parameters y_0, a and b were
334 obtained from a least-squares adjustment to monthly synthetic R_h data obtained by
335 summing up simulations of half-hourly R_h computed as in *Lloyd and Taylor* [1994] and
336 using the 10-year temperature records of the old jack pine stand obtained from the
337 Fluxnet-Canada / Canadian Carbon Program Data Information System.
338 The strength of this modelling approach is supported by the good performance of
339 StandLEAP in a comparison of its simulation results with measurements by eddy-flux
340 towers of GPP [data from Fluxnet-Canada, *Margolis et al*., 2006], ecosystem respiration
341 (Re) and NEP from 2000 to 2006 in a 95-year-old stand in Saskatchewan, Canada (Fig.
342 3). The model captured reasonably well the month-to-month variability in these variables
343 (GPP-R^2 = 0.92; Re-R^2 = 0.92; NEP-R^2 = 0.63; n = 84 months). The capacity of
344 FineLEAP to simulate canopy-level gas exchanges has also been verified by comparing

hourly [*Bernier et al.*, 2001] and daily [*Raulier et al.*, 2002] measurements of plot-level transpiration to simulated values for two different stands of sugar maple (*Acer saccharum* Marsh.).

4.3 Statistical analyses

Tree-ring width measurements in boreal forests have an autocorrelation structure that can be expressed as an auto-regressive (AR) process of order *p*:

[eq. 8] $I_t = \phi I_{t-p} + ... + \phi_1 I_{t-1} + e_t$,

where I_t are the tree-ring width measurements for year *t*, e_t are serially random inputs, and ϕ_i are the *p* autoregressive (AR) coefficients that produce the characteristic persistence seen in the tree rings [*Monserud*, 1986; *Biondi and Swetnam*, 1987; *Cook and Kairiukstis*, 1990; *Berninger et al.*, 2004]. A strong AR process will cause the tree-ring width measurements to be excessively smoothed, and vice versa. The AR process in tree rings reflects, amongst other things, how stored photosynthates are made available for growth in the following years. While this process can be mathematically described [*Misson*, 2004], its process basis remains difficult to express quantitatively so that one could predict empirically how much carbon produced a given month or year should be allocated to the growth in the following years [i.e. *Kagawa et al.*, 2006]. The autocorrelation function in TGI can indeed go beyond an AR1 process [*Monserud*, 1986].

In contrast, there is no such year-to-year carry-over in yearly totals of simulated NPP by StandLEAP. In order to correct for this deficit and make the comparison of NPP

368 and TGI possible, the two series must be brought to a similar AR process. In this study,
369 we estimated the AR process of the jack pine TGI and applied the AR equation
370 parameters [*Cook and Kariukstis*, 1990] to the standardized yearly totals of simulated
371 NPP, which were obtained by dividing annual NPP values by the long-term mean of NPP
372 over 1912–2000. We hereafter refer to this new NPP series as the NPP^{AR} series. The
373 application of this transformation to NPP does not violate the assumption of
374 independence between the two datasets, but allows them to have a similar time-dependent
375 (or 'smoothing') behaviour. Another approach would have been to remove the AR
376 process in TGI through auto-regressive modeling (i.e. prewhitening). This, however,
377 would have resulted in a significant loss of low-frequency changes in the TGI [for
378 analyses of 'prewhitened' data, refer to *Girardin and Tardif*, 2005 and *Girardin et al.*,
379 2008]. The order of the autocorrelation process was determined using the Akaike
380 Information Criterion (AIC) implemented in the program ARSTAN (version 40c) [*Cook*
381 *and Krusic*, 2006].

382 Long-term linear changes in TGI, climatic, and simulated data were detected
383 using least-squares linear regressions [*von Storch and Zwiers*, 1999]. Goodness of fit was
384 described by the coefficient of determination (R^2). Significance of the slope was tested
385 against the null hypothesis that the trend is different from zero, using a variant of the *t*
386 test with an estimate of the effective sample size that takes into account the presence of
387 serial persistence (red noise bias) in data [*von Storch and Zwiers*, 1999; their sections
388 8.2.3 and 6.6.8]. For those time-series having an autocorrelation structure expressed as an
389 AR process of order greater than one (AR > 1), the significance of trends was evaluated
390 using Monte Carlo simulations. In this analysis, 1000 random time series with similar

391 autocorrelation structure as the original data were tested for the presence of trends and
392 99%, 95% and 90% percentiles of the coefficient of determination were collected and
393 used as a criterion for testing against the null hypothesis. When necessary, data were
394 ranked prior to analysis to satisfy the normality distribution requirement in model
395 residuals [*von Storch and Zwiers*, 1999]. The period of analysis for this study was
396 1912–2000 (e.g. limited to the earliest year of meteorological data and the latest year
397 covered by tree-ring data).

398 As mentioned earlier, the StandLEAP simulator does not incorporate CO_2
399 enhancement effects. In the event that a CO_2 fertilization effect has occurred during the
400 20th century, climatically driven simulations of NPP and TGI should show increasing
401 divergence with increasing or decreasing atmospheric CO_2 [*Graumlich*, 1991; *Jacoby and*
402 *D'Arrigo*, 1989; 1997; *Rathgeber et al.*, 2000]. To test this fertilization hypothesis,
403 residuals of the difference between TGI and NPP^{AR} were related to atmospheric CO_2 data
404 using correlation analysis and piecewise regression [*Friedman*, 1991]. In the regression
405 analysis, the relationship between residuals and [CO_2] was described by a series of linear
406 segments of differing slopes, each of which was fitted using a basis function. Breaks
407 between segments were defined by a knot in a model that initially over-fitted the data,
408 and was then simplified using a backward/forward stepwise cross-validation procedure.
409 This approach was preferred over a linear trend analysis because CO_2 increases non-
410 linearly through time. The null hypothesis H_o of 'no fertilization effect' was to be rejected
411 in the presence of a basis function with a positive slope post-1970 (i.e. when the rate of
412 CO_2 increase was most important). The R package 'earth' was used [*R Development Core*
413 *Team*, 2007]. The Generalized Cross Validation (GCV) penalty per knot was set to four

414 and the minimum amount of observations between knots was set to 25 to ensure
415 numerical stability. Other parameters were kept as in the 'earth' default settings.
416

417 4.4 Sensitivity analysis to atmospheric CO_2

418 Empirical evidence indicating CO_2 fertilization effects has often resulted from laboratory
419 or controlled experiments following a doubling of pre-industrial CO_2 concentrations from
420 approximately 300 ppmv to 700 ppmv [e.g. *Norby et al.*, 2005]. The CO_2 forcing acting
421 on natural environments is much lower (from 300 ppmv in 1910 to 370 ppmv in 2000)
422 and, hence, the response of forests cannot be expected to be as large as the one seen in
423 experimental conditions [*Joos et al.*, 2002]. The fertilization effect in natural
424 environments could simply be under the limit of statistical detection [*D'Arrigo and*
425 *Jacoby*, 1993]. We investigated this potential source of error through a sensitivity
426 analysis in which an 'expected' effect of CO_2 fertilization was added to simulations of
427 NPP^{AR}. The 'expected' effect of CO_2 fertilization on forest growth is often quantified
428 using a logarithmic response function that takes the form of
429

430 [eq. 9] $$NPP_E = NPP_O \cdot (1 + \beta \ln(CO_{2E} / CO_{2O}))$$

431

432 where NPP_E and NPP_0 refer to net primary productivity (eq. 4) in enriched (CO_{2E}) and
433 control (CO_{2O}) CO_2 environments, respectively [e.g. *Friedlingstein et al.*, 1995;
434 *Rathgeber et al.*, 2000; *Peng et al.*, 2009]. In this equation, β is an empirical parameter
435 that ranges between 0.0 and 0.7, and is adjusted so that NPP under a doubled atmospheric
436 CO_2 concentration (from 350 to 700 ppmv) increases by approximately 23% (eq. 9)

437 [based on experimental evidence from *Norby et al.*, 2005]. We used a value of 0.34 for β,
438 as in *Peng et al.*, [2009]. Under the hypothesis that a fertilization effect in TGI has not
439 occurred, residuals of the difference between TGI and 'CO_2-enriched NPP^{AR}' simulations
440 should show a significant bias toward decreasing values with increasing atmospheric CO_2
441 (i.e. negative slope). On the other hand, a slope that is not significantly different from
442 zero would imply that the fertilization effect in TGI is possible but too small to be
443 statistically detected by our modelling procedure. In such an eventuality, the CO_2
444 fertilization effect could simply be masked by the high inter-annual variability in the TGI
445 time-series.
446

447 5. Results

448 5.1 Temporal changes in tree growth index

449 Most sampled jack pine trees originated from post-fire recruitment episodes, as for
450 example in the 1890s (~60% of trees) and 1750s to 1770s (~20%) (Fig. 4b). The only
451 information available on growth conditions prior to the 1890s was from dead trees. That
452 being said, a close relationship between average ring width of dead and living trees and
453 tree age (Fig. 5) (R^2 = 0.49; n = 332) suggested the existence of relatively homogeneous
454 behaviour in the tree population under study with regard to growth rates. Also, the age-
455 related growth trend of trees originating from prior to 1880 was reasonably similar in
456 level and slope to a curve obtained from trees originating after 1880 (Figs. 2b). We also
457 found little difference in the age-related growth trends under different classes of jack pine
458 dominance (auxiliary material Fig. S4). Therefore, one can assume that the trees belonged

459 to the same population, a prerequisite for application of the regional curve standardization
460 [*Esper et al.*, 2003].

461 First-order autocorrelation (AR1) of the jack pine record was 0.83 over 1717–
462 2000, reflecting high biological memory (i.e. persistence of previous year growth
463 conditions). The best AR model fit was obtained using an AR(5) process. However, an
464 AR(2) model (described in Table 1) was considered the best for a sub-period covering
465 1880–2000.

466 Expressed population signal (EPS) values meet signal strength acceptance for the
467 full period covered by tree-ring data (Fig. 4d). Replication of ring-width measurements
468 may thus be considered sufficiently high to approximate a signal representative of a
469 theoretical population of an infinite number of trees, i.e. an entire forest stand [*Wigley et*
470 *al.*, 1984]. However, the low correlation obtained during the 30-year 'moving window'
471 analysis of the inter-series correlation ($Rbar < 0.32$ over much of the 19th and 20th
472 centuries; Fig. 4d) demonstrates the high variability among measurement series, and
473 suggests the action of diverse biological and non-biological forcing agents on the growth
474 of the jack pine trees. This was further highlighted by a wide bootstrap confidence
475 interval around the mean throughout much of the 19th century, when sampling replication
476 was low (Fig. 4a). As opposed to any previous time periods, the period submitted to our
477 modelling experiment (i.e. 1912–2000) appeared minimally biased, as can be assessed
478 from high EPS, relatively stable *Rbar*, and a narrow confidence interval around the mean.
479 The final TGI chronology suggested marked variations in the growth of jack pine trees,
480 with low growth from the 1910s to 1940 and around 1960, and highs in the 1950s and
481 post 1970 (Fig. 4a). Least-squares linear regression applied to the TGI indicated a

positive trend over 1912–2000 (Table 2). The trend explained 34.4% of the variance in data (Table 2).

5.2 Simulated forest productivity

Simulated annual GPP over 1912–2000 averaged 857 gC m^{-2} yr^{-1}, and simulated respiration losses were about 52% of this amount (Fig. 6). Annual simulated NPP averaged 460 gC m^{-2} yr^{-1}, with a minimum of 212 gC m^{-2} yr^{-1} in 1961 and a maximum of 556 gC m^{-2} yr^{-1} in 1977 (Fig. 7). About 60% of annual NPP was produced during the June to August period (average equals 270 gC m^{-2} yr^{-1}). Summer NPP also showed a higher departure from the mean (standard deviation of 45 gC m^{-2} yr^{-1}) than spring or fall (respectively 21 and 15 gC m^{-2} yr^{-1}). Indeed, except perhaps in the 1970-80s, most of the highs and lows in annual NPP (Fig. 7) were found within the productivity during summer months. These variations were driven in the model by the climate modifiers affecting RUE (eq. 2) and, hence, GPP. The temperature constraints on respiration (eq. 4) were likely not sufficiently important to induce in NPP the large departures from the mean seen in Fig. 7.

The simulation suggested an increase in forest productivity over the century, with an increase of annual GPP estimated at 0.780 gC m^{-2} yr^{-1} and a linear trend explaining 9.7% of the variance in data (Table 2; Fig. 6). Nevertheless, carbon losses due to respiration have also significantly increased, but such losses were more than compensated by increased GPP, resulting in a significant rise in NPP of 0.502 gC m^{-2} yr^{-1}. This rise in NPP explained 7.8% of the variance in data (Table 2; Fig. 7). Most of the increase was simulated to have taken place in the spring (by 0.233 gC m^{-2} yr^{-1}).

505 Climate factors encapsulated in the bioclimatic model were also tested for the
506 presence of linear trends. Amongst factors that could explain the simulated upward trend
507 in forest productivity were increases in the length of the growing seasons, as inferred
508 from the annual sums of growing degree days above 5°C, and increased availability of
509 soil moisture in the first meter of soil (Table 2 and Fig. 8). Both variables had a
510 significant positive trend over 1912–2000 ($P < 0.05$), explaining 6.0% and 6.8% of the
511 variance in data, respectively.
512

513 5.3 Comparing empirical data with simulations

514 The AR process dominating the jack pine TGI (Table 1) was applied to the yearly totals
515 of simulated NPP so that both series could share similar time-dependent behaviour (see
516 Methods). The two records, illustrated in Fig. 9a, shared 47.2% of common variance over
517 their common period of analysis, i.e. 1912 to 2000 ($P < 0.01$ according to Monte Carlo
518 simulations). The amount of shared variance equalled 28.5% ($P < 0.05$) when both series
519 were detrended prior to analysis. Most often, the simulation of NPP^{AR} propagated well
520 within the uncertainty band of the TGI data (Fig. 9). Nevertheless, the simulation did not
521 do well in 1921–1925 (overestimation), 1936–1937 (underestimation), 1975–1976
522 (underestimation), and 1992 (overestimation). These years were not found to be
523 systematically related to a climatic factor (as investigated with Student-t tests on monthly
524 climatic data) or to a biological agent acting on growth, such as outbreaks of the jack pine
525 budworm (*Choristoneura pinus* Freeman) [*McCullough*, 2000; *Volney*, 1988] recorded in
526 the DMPF from 1938 to 1942 and in 1985 [*Canadian Forestry Service*, 1986]. These
527 years might reflect the influence of climatic extremes not taken into account by the

528 simulator or of magnitudes outside the domain of calibration of the modifiers affecting
529 RUE (see Methods). If we eliminate the 'disconnected' years 1936 and 1976 (with
530 Studentized residuals > 3.0) from the data comparison, the amount of shared variance
531 between data rises to 59.0% (39.5% after detrending).

532 A positive trend in productivity over the past century is clearly distinguishable in
533 the NPP^{AR} simulations and in TGI (Table 2 and Fig. 9), indicating long-term changes in
534 growing conditions. Both TGI and NPP^{AR} shared similar regression slopes (i.e. no
535 statistical difference) and amount of variance explained by the trend line (Table 2). Also
536 clearly distinguishable in the jack pine TGI series were growth declines in the 1920s to
537 1930s and early 1960s (Fig. 9a). Coincident with these episodes are notable drought
538 events that are reflected in the index of available soil water at a depth of 1 m (Fig. 8b).
539 The influence of moisture availability on jack pine growth was readily apparent when
540 correlating the TGI data over 1912–2000 with the smoothed version of available soil
541 water (Fig. 8b): the two records shared 42.7% of variance.

542

543 5.4 Testing for a CO_2 fertilization effect

544 Climatically driven simulations of NPP^{AR} and TGI did not show evidence of increasing
545 divergence with increasing atmospheric [CO_2] as residuals of the difference between TGI
546 and NPP^{AR} (Fig. 10a) were uncorrelated to long-term changes in the atmospheric [CO_2]
547 ($R^2 = 0.017$, $P > 0.30$). In addition, the piecewise regression model did not detect a linear
548 segment or a long-term trend in residuals capturing a missing effect of increasing
549 atmospheric [CO_2] on NPP (Fig. 10a). When the effect of CO_2 fertilization was added to
550 NPP through the use of eq. 9 and $\beta = 0.34$, the residuals of the difference between TGI

551 and CO_2-enriched NPP^{AR} were negatively correlated to long-term changes in the
552 atmospheric CO_2 ($R^2 = 0.067$, $P < 0.05$), and presented a significant bias according to the
553 piecewise regression analysis (Fig. 10b). Our results therefore suggest that long-term
554 changes in the TGI were adequately reproduced by the climatically driven simulation of
555 NPP^{AR} without inclusion of a CO_2 factor.

556 We also conducted a sensitivity analysis in order to evaluate the statistical
557 detection limit of our approach. Our analysis involved re-doing the simulation of NPP^{AR}
558 with values of β varying between 0 and 0.7. Results of this analysis revealed that values
559 of β greater than 0.20 generated an overestimation of the slope of the linear trend between
560 NPP^{AR} and TGI data (period 1912–2000) (Fig. 11a). Residuals between NPP^{AR} and TGI
561 also increased with values of β greater than 0.20 (Fig. 11b) and were increasingly
562 correlated to CO_2 (Fig. 11c). A cut-off value of $\beta = 0.20$ corresponded to a growth
563 enhancement of 14% with a doubling of CO_2. We also found a slight improvement of
564 model fit between TGI and NPP^{AR} with the addition of a weak CO_2 factor between 0.10
565 and 0.15, but this effect was non-significant (see minimum value in Fig. 11b and
566 auxiliary material Figs. S5 and S6).

567

568 6. Discussion

569 It is of increasingly common practice for modellers to include CO_2 fertilization effects
570 when assessing the current and future impacts of global climate change (see
571 Introduction). This practice, which is done using empirical evidence from laboratory or
572 controlled conditions, is often applied to large territories (e.g. continental scale) and over
573 a range of habitats and species. Within the detection limit of the data-model approach

574 used in this work, we find nothing to support the idea of a FACE-level CO_2 growth
575 enhancement (23% for a doubling of CO_2) in jack pine trees of the DMPF during the 20th
576 century ($\beta = 0.34$). In addition, comparison between recent growth and growth prior to
577 the 1890s in our jack pine TGI series of the DMPF fails to show the multicentury
578 increase in growth that should be expected as a result of the CO_2 fertilization effect
579 [*Jacoby and D'Arrigo*, 1989, 1997; *Huang et al.*, 2007]. As seen in Fig. 2, the age-related
580 growth trend of trees originating after 1880 is reasonably similar in level and slope to a
581 curve obtained from trees originating prior to 1880 in spite of significant increases in
582 atmospheric CO_2 over the past century [*Keeling et al.*, 1982; *Etheridge et al.*, 1996].
583 Because of the detection limit of our approach, evaluated at 14% growth enhancement for
584 a doubling of CO_2 (maximum $\beta = 0.20$), our results do not invalidate suggestions for a
585 lower CO_2 fertilization effect, such as the value of 15% proposed by *Hickler et al.* [2008].
586 Our results do suggest the need to use caution when including CO_2 fertilization effects in
587 models.

588 Empirical observations provide support to the correctness of our modelling results
589 with respect to the factors driving the simulated 20th century increase in NPP. Net
590 ecosystem productivity of coniferous forests is increased by early spring warming [*Arain*
591 *et al.*, 2002; *Grant et al.*, 2009] but reduced by hot summers and soil moisture depletion
592 [*Griffis et al.*, 2003; *Dunn et al.*, 2007]. The pattern of year-to-year changes in tree
593 growth reflects the underlying influences of variability in the climate and occurrence rate
594 of weather episodes favourable or not to photosynthesis (eq. 1) and respiration (eq. 4).
595 Our observed trends toward greater length of the growing season and greater available
596 soil water are consistent with these short-term observations. Notably, springtime

increases in simulated NPP suggest that growth conditions in the second half of the century have benefited from increasing growing season degree-days, particularly through an earlier onset of spring (Fig. 7). Extension of the growing season by up to 2 weeks in mid- and high northern latitudes since the early 1970s is apparent in remotely-sensed vegetation indices (NDVI) [*Myneni et al.*, 1997; *Zhou et al.*, 2001] and in seasonal trends of atmospheric CO_2 drawdown [*Keeling et al.*, 1996]. The positive influence of global warming on plant growth and establishment in high-latitude, cold-limited systems has widely been reported [e.g. *Jacoby and D'Arrigo*, 1989, 1997; *Gamache and Payette*, 2004; *Briffa et al.*, 2008].

Also clearly distinguishable in the jack pine TGI series of the DMPF were growth declines in the 1920s to 1930s and early 1960s coherent with intense or frequent drought years. These well-documented droughts [e.g. *Girardin and Wotton*, 2009] may have been relatively mild when examined in the context of past centuries [e.g. *Cook et al.*, 2004], but the 'Dust Bowl' drought nevertheless severely affected almost two-thirds of the United States and parts of Mexico and Canada during the 1930s [*Schubert et al.*, 2004]. It is apparent from our NPP simulations and empirical data that carbon uptake by the jack pine population of the DMPF was severely limited for much of the early 20th century as a consequence of this extreme climatic anomaly. The year 1961, which was referred to by *Girardin and Wotton* [2009] as the driest summer over the period 1901–2002 for Canada as a whole, also stands out as the year with the lowest simulated NPP (and measured TGI) for the entire simulated period.

So why has CO_2 fertilization of jack pine trees in the DMPF failed to be detected? It is apparent that constraints other than atmospheric CO_2 concentration have been and

620 are still limiting the growth of this forest. Temperature effects on growth are strongly
621 mediated by nutrient availability and capture [*Jarvis and Linder*, 2000]. Although the
622 drop in forest productivity with increasing latitude highlights the primary controlling role
623 of climate across the spatial domain (e.g. temperature dependence of the CO_2-
624 enhancement effect as discussed in the Introduction), secondary factors, such as soil
625 fertility and stand age, that operate on a longer time lag may be attenuating the immediate
626 impact of climate warming and CO_2 fertilization in these forests [e.g. *Körner et al.*,
627 2005]. One constraint would be the insufficient availability of nitrogen in soils to meet
628 the increasing demand under elevated CO_2 [*Oren et al.*, 2001; *Johnson et al.*, 2004;
629 *Norby et al.*, 2008, 2009], particularly on sites with low to moderate soil nitrogen
630 availability [*Reich et al.*, 2006]. In general, coniferous forests are believed to have lower
631 availability of nitrogen due to slower nutrient turnover than deciduous forests [*Jerabkova*
632 *et al.*, 2005; *Ste-Marie et al.*, 2007].

633 An additional constraint on the detection of the CO_2 fertilization effect is the
634 expected size of this effect in comparison to the detection limit. The effect may not yet be
635 detectable in natural forest environment, in part because it may be much smaller than
636 what is found in controlled experiments, and in part because the CO_2 increases during the
637 studied interval were relatively modest, again in comparison to controlled experiments.
638 These findings concur with those of *Joos et al.* [2002]. The results of the sensitivity
639 analysis revealed that our analysis cannot detect a fertilization effect of up to $\beta = 0.20$,
640 which corresponds to a growth enhancement of 14% with a doubling of CO_2. However,
641 this value of β as a detection cut-off results in part from our choice of pre-treatment
642 method for the TGI measurement series that retained the most amount of trend possible

643 (auxiliary material Fig. S1). This choice enhances the probability of generating false
644 positive or Type 1 errors at lower values of β (i.e. accept the fertilization hypothesis when
645 in fact there is none). The use of other detrending methods would have resulted in a
646 detection cut-off value of β lower than 0.20 (auxiliary material Fig. S6).

647 Other uncertainties may also weaken our inference. In particular, the method
648 relies on the use of a dataset with a uniform distribution of tree establishment and
649 mortality dates over time in order to allow common climate/CO_2 signals to be cancelled
650 and averaged out when the series are aligned by cambial age (Fig. 3a). In our
651 experimentation this condition is not necessarily met as a large proportion of trees
652 germinated within a short period in the 1890s. Nonetheless, results of a sensitivity
653 analysis (auxiliary material Fig. S2) that involved a downsampling of the number of trees
654 established during that interval suggest that our inference is robust against this source of
655 error. Finally, the instrumental weather data used as input for the simulator were subject
656 to homogenization and this could induce some uncertainty in the measurement trend,
657 which might also be carried over into the modeled estimates. In our estimation, however,
658 none of these sources of uncertainty weaken the basic inference from this study that, in
659 our boreal forest environment, we could not detect the level of CO_2 fertilization effect
660 that has been reported in controlled FACE experiments [*Norby et al.*, 2005] and that is
661 often included in simulations of future forest productivity [e.g. *Chen et al.*, 2000; *Peng et*
662 *al.,* 2009].

663

664 7. Concluding remarks

665 This study suggests that empirical evidence from controlled experiments on CO_2
666 fertilization cannot be directly extrapolated to large forested areas without a good
667 understanding of local constraints on forest growth. Inclusion of such additional
668 constraints on growth in the models remains a daunting task when they are to be applied
669 to large heterogeneous landscapes such as the boreal forest. Adding complexity to models
670 without empirical supporting evidence as to the applicability of the additional
671 relationships may in the end become counter-productive and generate unrealistic
672 projections of future forest states. In spite of all their shortcomings, field-based studies
673 such as this one remain one of the best guarantees that we indeed understand forest
674 growth and can adequately predict its future.

675 We currently do not know if our inference with respect to the absence of long-
676 term CO_2 fertilization applies to all of Canada's closed-canopy boreal region but
677 widespread replication of this type of study is currently challenging. The technique
678 employed in the processing of our jack pine tree-ring data (regional curve
679 standardization) has high capabilities for preserving long-term growth changes [e.g.
680 *D'Arrigo et al.*, 2006]. Nevertheless, the technique can only be applied in specific
681 circumstances [*Esper et al.*, 2003] and requires high within-site replication (*D'Arrigo et*
682 *al.*, 2006). Many tree-ring datasets across closed-canopy forests of boreal Canada have
683 been developed in the past [*Girardin et al.*, 2006; *St. George et al.*, 2009]. However, few
684 of these data have been collected from productive forests following a dense sampling
685 scheme that includes sampling of multiple age cohorts. Expansion of this work is further
686 limited by the absence of plot-level data necessary to run process-based models on stands
687 in which growth increment data were collected. While the applicability of species-

688 specific process-based models may be fairly narrow in scale owing to the complexity of
689 input data, they are of valuable help in answering specific questions that are relevant to
690 modellers of carbon exchanges of broad spatial scales. Estimates of stand attributes, such
691 as biomass and soil types, through remote sensing could help address some of these
692 issues in the future. There is, however, clearly a need for additional tree-ring sampling
693 campaigns coupled with complete plot-level information if we are to successfully
694 document and attribute long-term growth trends in the circumboreal forests.
695

696 Acknowledgements

697 Funds for this research were provided by the Canadian Forest Service operating budgets,
698 the Canada Research Chairs Program, the Natural Sciences and Engineering Research
699 Council of Canada and the University of Winnipeg. Special thanks are extended to Allan
700 Barr and to Fluxnet-Canada / Canadian Carbon Program and associated funding agencies
701 for the generation and provision of eddy-flux tower measurements. We thank Mike
702 Lavigne, Dennis Baldocchi, the Associate Editor, Mark J. Ducey, Greg King, Flurin
703 Babst, and an anonymous reviewer for providing valuable comments on an earlier draft
704 of this manuscript.
705

706 References

707 Aber, J. D., and C. A. Federer (1992), A generalized, lumped-parameter model of
708 photosynthesis, evapotranspiration and net primary production in temperate and
709 boreal forest ecosystems, *Oecologia*, *92*, 463–474.

710 Aber, J. D., S. V. Ollinger, C. A. Federer, P. B. Reich, M. L. Goulden, D. W. Kicklighter,
711 J. M. Melillo, and R. G. Lathrop Jr. (1995), Predicting the effects of climate change
712 on water yield and forest production in the northeastern United States, *Clim. Res.*, *5*,
713 207–222.
714 Agren, G. I., and B. Axelsson (1980), Population respiration: a theoretical approach,
715 *Ecol. Model.*, *11*, 39–54
716 Ainsworth, E. A., and S. P. Long (2005), What have we learned from 15 years of free-air
717 CO_2 enrichment (FACE)? A meta-analytic review of the responses of
718 photosynthesis, canopy properties and plant production to rising CO_2, *New Phytol.*,
719 *165*, 351–372.
720 Arain, M. A., T. A. Black, A. G. Barr, P. G. Jarvis, J. M. Massheder, D. L. Verseghy, and
721 Z. Nesic (2002), Effects of seasonal and interannual climate variability on net
722 ecosystem productivity of boreal deciduous and conifer forests, *Can. J. For. Res.*,
723 *32*, 878–891.
724 Baldocchi, D. D. (2003), Assessing the eddy covariance technique for evaluating carbon
725 dioxide exchange rates of ecosystems: past, present and future, *Glob. Change Biol.*,
726 *9*, 479–492.
727 Baldocchi, D., et al. (2001), FLUXNET: A new tool to study the temporal and spatial
728 variability of ecosystem-scale carbon dioxide, water vapor, and energy flux
729 densities, *Bull. Am. Meteorol. Soc.*, *82*, 2415–2435.
730 Balshi, M. S., et al. (2007), The role of historical fire disturbance in the carbon dynamics
731 of the pan-boreal region: A process-based analysis, *J. Geophys. Res.*, *112*, G02029,
732 doi:10.1029/2006JG000380.

733 Bernier, P. Y., F. Raulier, P. Stenberg, and C.-H. Ung (2001), Importance of needle age
734 and shoot structure on canopy net photosynthesis of balsam fir (*Abies balsamea*): a
735 spatially inexplicit modeling analysis, *Tree Physiol.*, *21*, 815–830.
736 Bernier, P. Y., N. Bréda, A. Granier, F. Raulier, and F. Mathieu (2002), Validation of a
737 canopy gas exchange model and derivation of a soil water modifier for transpiration
738 for sugar maple (*Acer saccharum* Marsh.) using sap flow density measurements,
739 *For. Ecol. Manag.*, *163*, 185–196.
740 Berninger, F., P. Hari, E. Nikinmaa, M. Lindholm, and J. Meriläinen (2004), Use of
741 modeled photosynthesis and decomposition to describe tree growth at the northern
742 tree line, *Tree Physiol.*, *24*, 193-204.
743 Biondi, F., and T. W. Swetnam (1987), Box-Jenkins models of forest interior tree-ring
744 chronologies, *Tree-Ring Bull.*, *47*, 71–96.
745 Briffa, K. R., and T. M. Melvin (in press), A closer look at Regional Curve
746 Standardisation of tree-ring records: justification of the need, a warning of some
747 pitfalls, and suggested improvements in its application, *Dendroclimatology:*
748 *Progress and Prospects*, Series: Developments in Paleoenvironmental Research,
749 edited by M. K. Hughes, H. F. Diaz, and T. W. Swetnam, Springer Verlag.
750 Briffa, K. R., V. V. Shishov, T. M. Melvin, E. A. Vaganov, H. Grudd, R. M. Hantemirov,
751 M. Eronen, and M. M. Naurzbaev (2008), Trends in recent temperature and radial
752 tree growth spanning 2000 years across northwest Eurasia, *Philos. Trans. R. Soc.*
753 *Lond. B. Biol. Sci.*, *363*, 2271–2284.
754 Canadian Forestry Service (1986), Forest insect and disease survey reports, Edmonton,
755 Alberta.

Caspersen, J. P., S. W. Pacala, J. C. Jenkins, G. C. Hurtt, P. R. Moorcroft, and R. A. Birdsey (2000), Contributions of land-use history to carbon accumulation in U.S. forests, *Science*, *290*, 1148–1151.

Chen, J. M., W. Chen, J. Liu, and J. Cihlar (2000), Annual carbon balance of Canada's forests during 1895–1996, *Global Biogeochem. Cycles*, *14*, 839–850.

Cook, E. R., and L. A. Kairiukstis (1990), *Methods of dendrochronology: applications in the environmental sciences*, 408 pp., Kluwer Academic Publishers, Boston, MA, USA.

Cook, E. R., C. A. Woodhouse, C. M. Eakin, D. M. Meko, and D. W. Stahle (2004), Long-term aridity changes in the western United States, *Science*, *306*, 1015–1018.

Cook, E. D., and P. J. Krusic (2006), Program ARSTAN 40c. Tree-ring Laboratory, Lamont-Doherty Earth Observatory, Palisades, NY.

Crous, K. Y., M. B. Walters, and D. S. Ellsworth (2008), Elevated CO_2 concentration affects leaf photosynthesis-nitrogen relationships in *Pinus taeda* over nine years in FACE. *Tree Physiol*., *28*, 607–614.

D'Arrigo, R., and G. C. Jacoby (1993), Tree growth-climate relationships at the northern boreal forest tree line of North America: evaluation of potential response to increasing carbon dioxide, *Glob. Biogeochem. Cycles*, *7*, 525–535.

D'Arrigo, R., R. Wilson, and G. Jacoby (2006), On the long-term context for late twentieth century warming, *J. Geophys. Res.*, *111*, D03103, doi:10.1029/2005JD006352.

777 Dunn, A. L., C. C. Barford, S. C. Wofsy, M. L. Goulden, and B. C. Daube (2007), A long
778 term record of carbon exchange in a boreal black spruce forest: means, responses to
779 interannual variability, and decadal trends, *Glob. Change Biol.*, *13*, 577–590.
780 Eguchi, N., K. Karatsu, T. Ueda, R. Funada, K. Takagi, T. Hiura, K. Sasa, and T. Koike
781 (2008), Photosynthetic responses of birch and alder saplings grown in a free air CO_2
782 enrichment system in northern Japan. *Trees, 22*, 437–447.
783 Esper, J., E. R. Cook, P. J. Krusic, K. Peters, and F. H. Schweingruber (2003), Tests of
784 the RCS method for preserving low-frequency variability in long tree-ring
785 chronologies, *Tree-Ring Res.*, *59*, 81–98.
786 Etheridge, D. M., L. P. Steele, R. L. Langenfelds, R. J. Francey, J.-M. Barnola, and V. I.
787 Morgan (1996), Natural and anthropogenic changes in atmospheric CO_2 over the
788 last 1000 years from air in Antarctic ice and firn, *J. Geophys. Res.*, *101*, 4115–4128.
789 Farquhar, G. D., S. von Caemmerer, and J. A. Berry (1980), A biochemical model of
790 photosynthetic CO_2 assimilation in leaves of C_3 species, *Planta*, *149*, 78–90.
791 Friedlingstein, P., I. Fung, E. Holland, J. John, G. Brasseur, D. Erickson, D. Schimel
792 (1995), On the contribution of CO_2 fertilization to the missing biospheric sink,
793 *Global Biogeochem. Cycles*, *9*, 541–556.
794 Friedman, J. H. (1991), Multivariate adaptive regression splines, *Ann. Stat., 19*, 1–67.
795 Fritts, H. C. (1976), Tree rings and climate. The Blackburn Press. Caldwell, NJ. 567 pp.
796 Gamache, I., and S. Payette (2004) Height growth response of tree line black spruce to
797 recent climate warming across the forest-tundra of eastern Canada, *J. Ecol.*, *92*,
798 835–845.

799 Girardin, M.-P., and J. Tardif (2005), Sensitivity of tree growth to the atmospheric
800 vertical profile in the Boreal Plains of Manitoba, Canada, *Can. J. For. Res.*, *35*, 48–
801 64.
802 Girardin, M. P., and B. M. Wotton (2009), Summer moisture and wildfire risks across
803 Canada. *J. Appl. Meteorol. Climatol.*, *48*, 517–533.
804 Girardin, M. P., F. Raulier, P. Y. Bernier, and J. C. Tardif (2008), Response of tree
805 growth to a changing climate in boreal central Canada: a comparison of empirical,
806 process-based, and hybrid modelling approaches, *Ecol. Model.*, *213*, 209–228.
807 Girardin, M.-P., J. C. Tardif, M. D. Flannigan, and Y. Bergeron (2006), Synoptic-scale
808 atmospheric circulation and boreal Canada summer drought variability of the past
809 three centuries. *J. Climate*, *19*, 1922–1947.
810 Gower, S. T., J. G. Vogel, J. M. Norman, C. J. Kucharik, S. J. Steele, and T. K. Stow
811 (1997), Carbon distribution and aboveground net primary production in aspen, jack
812 pine, and black spruce stands in Saskatchewan and Manitoba, Canada. *J. Geophys.*
813 *Res.*, *102*, 29029–29041.
814 Grant, R. F., H. A. Margolis, A. G. Barr, T. A. Black, A. L. Dunn, P. Y. Bernier, and O.
815 Bergeron (2009), Changes in net ecosystem productivity of boreal black spruce
816 stands in response to changes in temperature at diurnal and seasonal time scales,
817 *Tree Physiol.*, *29*, 1–17.
818 Graumlich, L. J. (1991), Subalpine tree growth, climate, and increasing CO_2: an
819 assessment of recent growth trends, *Ecology*, *72*, 1–11.

820 Griffis, T. J., T. A. Black, K. Morgenstern, A. G. Barr, Z. Nesic, G. B. Drewitt, D.
821 Gaumont-Guay, and J. H. McCaughey (2003), Ecophysiological controls on the
822 carbon balances of three southern boreal forests, *Agric. For. Meteorol.*, *117*, 53–71.
823 Hänninen, H. (1990), Modelling bud dormancy release in trees from cool and temperate
824 regions. *Acta For. Fenn.*, *213*, 1–47.
825 Hickler T., B. Smith, I. C. Prentice, K. Mjofors, P. Miller, A. Arneth, and M. T. Sykes
826 (2008), CO_2 fertilization in temperate FACE experiments not representative of
827 boreal and tropical forests, *Glob. Change Biol.*, *14*, 1531–1542 doi: 10.1111/j.1365-
828 2486.2008.01598.x
829 Holmes, R. L. (1983), Computer-assisted quality control in tree-ring dating and
830 measurement, *Tree-Ring Bull.*, *43*, 69–78.
831 Huang, J.-G., Y. Bergeron, B. Denneler, F. Berninger, and J. Tardif (2007), Response of
832 forest trees to increased atmospheric CO_2. *Crit. Rev. Plant Sci.*, *26*, 265–283.
833 Hunt Jr., E. R., F. C. Martin, and S. W. Running (1991), Simulating the effects of climate
834 variation on stem carbon accumulation of a ponderosa pine stand: comparison with
835 annual growth increment data. *Tree Physiol.*, *9*, 161–171.
836 Jacoby, G. C., and R. D'Arrigo (1989), Reconstructed Northern Hemisphere annual
837 temperature since 1671 based on high-latitude tree-ring data from North America,
838 *Clim. Change*, *14*, 39–59.
839 Jacoby, G. C., and R. D. D'Arrigo (1997), Tree rings, carbon dioxide, and climatic
840 change, *Proc. Natl. Acad. Sci. USA*, *94*, 8350–8353.
841 Jarvis, P., and and S. Linder (2000), Constraints to growth of boreal forests, *Nature*, *405*,
842 904–905.

843 Jerabkova, L., C. E. Prescott, and B. E. Kishchuk (2005), Nitrogen availability in soil and
844 forest floor of contrasting types of boreal mixedwood forests, *Can. J. For. Res.*, *36*,
845 112–122.
846 Johnson, D. W., W. Cheng, J. D. Joslin, R. J. Norby, N. T. Edwards, and D. E. Todd
847 (2004), Effects of elevated CO_2 on nutrient cycling in a sweetgum plantation.
848 *Biogeochemistry*, *69*, 379–403.
849 Joos, F., I. C. Prentice, and J. I. House (2002), Growth enhancement due to global
850 atmospheric change as predicted by terrestrial ecosystem models: consistent with
851 US forest inventory data, *Glob. Change Biol.*, *8*, 299–303.
852 Kagawa, A., A. Sugimoto, and T. C. Maximov (2006), $^{13}CO_2$ pulse-labelling of
853 photoassimilates reveals carbon allocation within and between tree rings, *Plant Cell*
854 *Environ.*, *29*, 1571–1584.
855 Keeling, C. D., R. B. Bacastow, and T. P.Whorf (1982), Measurements of the
856 concentration of carbon dioxide at Mauna Loa Observatory, Hawaii, Carbon
857 Dioxide Review: 1982, edited by W. C. Clarke, Oxford University Press, New
858 York.
859 Keeling, C. D., J. F. S. Chin, and T. P. Whorf (1996), Increased activity of northern
860 vegetation inferred from atmospheric CO_2 measurements, *Nature*, *382*, 146–149.
861 Körner C. H., J. Morgan, and R. Norby (2007), CO_2 fertilization: when, where, how
862 much? *Terrestrial ecosystems in a changing world series: Global change – The*
863 *IGBP series*, edited by J. G. Canadell, D. Pataki, and L. Pitelka, pp 9–21, Springer,
864 Berlin.

865 Körner, C., R. Asshoff, O. Bignucolo, H. Hättenschwiler, S. G. Keel, S. Peláez-Riedl, S.
866 Pepin, R. T. W. Siegwolf, and G. Zotz (2005) Carbon flux and growth in mature
867 deciduous forest trees exposed to elevated CO_2, *Science*, *309*, 1360–1362.
868 Lambert, M.-C., C.-H. Ung, and F. Raulier (2005), Canadian national tree aboveground
869 biomass equations, *Can. J. For. Res.*, *35*, 1996–2018.
870 Landsberg, J. J., and R. H. Waring (1997), A generalised model of forest productivity
871 using simplified concepts of radiation-use efficiency, carbon balance and
872 partitioning, *For. Ecol. Manag.*, *95*, 209–228.
873 Lavigne, M. B., and M. G. Ryan (1997), Growth and maintenance respiration rates of
874 aspen, black spruce and jack pine stems at northern and southern BOREAS sites,
875 *Tree Physiol.*, *17*, 543–551.
876 Leuning R., F. M. Kelliher, D. G. G. De Pury, and E. D. Schulze (1995), Leaf nitrogen,
877 photosynthesis, conductance and transpiration: scaling from leaves to canopies,
878 *Plant Cell Environ.*, *18*, 1183–1200.
879 Lloyd, J., and J. A. Taylor (1994), On the temperature dependence of soil respiration,
880 *Funct. Ecol.*, *8*, 315–323.
881 Margolis, H. A., L. B. Flanagan, and B. D. Amiro (2006), The Fluxnet-Canada Research
882 Network: Influence of climate and disturbance on carbon cycling in forests and
883 peatlands, *Agric. For. Meteorol.*, *140*, 1–5.
884 McCullough, D. G. (2000), A review of factors affecting the population dynamics of jack
885 pine budworm (*Choristoneura pinus pinus* Freeman), *Popul. Ecol.*, *42*, 243–256.
886 Mekis, E., and W. D. Hogg (1999), Rehabilitation and analysis of Canadian daily
887 precipitation time series. *Atmosphere-Ocean*, *37*, 53–85.

888 Misson, L. (2004), MAIDEN: a model for analyzing ecosystem processes in
889 dendroecology. *Can. J. For. Res.*, *34*, 874–887.
890 Misson, L., C. Rathgeber, and J. Guiot (2004) Dendroecological analysis of climatic
891 effects on *Quercus petraea* and *Pinus halepensis* radial growth using the process-
892 based MAIDEN model. *Can. J. For. Res.*, *34*, 888–898.
893 Monserud, R. A. (1986), Time-series analyses of tree-ring chronologies. *For. Sci.*, *32*,
894 349–372.
895 Myneni, R. B., C. D. Keeling, C. J. Tucker, G. Asrar, and R. R. Nemani (1997), Increased
896 plant growth in the northern high latitudes from 1981 to 1991, *Nature*, *386*, 698–
897 702.
898 Newcomer, J., et al. (2000), Collected data of the boreal ecosystem-atmosphere study.
899 CD-ROM. NASA, Goddard Space Flight Center, Greenbelt, MD.
900 Norby, R. J., S. D. Wullschleger, C. A. Gunderson, D. W. Johnson, and R. Ceulemans
901 (1999), Tree responses to rising CO_2 in field experiments: implications for the
902 future forest. *Plant Cell Environ.*, *22*, 683–714.
903 Norby, R. J., J. M. Warren, C. M. Iversen, B. E. Medlyn, R. E. McMurtrie, and F. M.
904 Hoffman (2008), Nitrogen limitation is reducing the enhancement of NPP by
905 elevated CO_2 in a deciduous forest. *Eos Trans. AGU*, 89(53), Fall Meet. Suppl.,
906 B32B–05.
907 Norby, R. J., et al. (2005), Forest response to elevated CO_2 is conserved across a broad
908 range of productivity. *Proc. Natl. Acad. Sci. USA*, *102*, 18052–18056.
909 Norby R. J., J. M. Warren, C. M. Iversen, C. T. Garten, B. E. Medlyn, and R. E.
910 McMurtrie (2009), CO_2 enhancement of forest productivity constrained by limited

911 nitrogen availability. *Nature Precedings*,
912 http://precedings.nature.com/documents/3747/version/1 (last consulted on 2010-06-
913 21).
914 Notaro, M., S. Vavrus, and Z. Liu (2007), Global vegetation and climate change due to
915 future increases in CO_2 as projected by a fully coupled model with dynamic
916 vegetation. *J. Climate*, *20*, 70–90.
917 O'ishi, R., A. Abe-Ouchi, I. C. Prentice, and S. Sitch (2009), Vegetation dynamics and
918 plant CO_2 responses as positive feedbacks in a greenhouse world, *Geophys. Res.*
919 *Lett.*, 36, L11706, doi:10.1029/2009GL038217.
920 Oren R,, et al. (2001), Soil fertility limits carbon sequestration by forest ecosystems in a
921 CO_2-enriched atmosphere, *Nature*, *411*, 469–472
922 Peng, C., X. Zhou, S. Zhao, X. Wang, B. Zhu, S. Piao, and J. Fang (2009), Quantifying
923 the response of forest carbon balance to future climate change in Northeastern
924 China: Model validation and prediction, *Global Planet. Change*, *66*, 179–194.
925 Prentice, I. C., and S. P. Harrison (2009), Ecosystem effects of CO_2 concentration:
926 evidence from past climates, *Clim. Past*, *5*, 297–307.
927 R Development Core Team (2007), 'R: a language and environment for statistical
928 computing', R Foundation for Statistical Computing. Vienna, Austria,
929 http://www.R-project.org.
930 Rathgeber, C., A. Nicault, J. Guiot, T. Keller, F. Guibal, and P. Roche (2000), Simulated
931 responses of *Pinus halepensis* forest productivity to climatic change and CO_2
932 increase using a statistical model, *Glob. Planet. Change*, *26*, 405–421.

933 Rathgeber, C., A. Nicault, J. O. Kaplan, and J. Guiot (2003), Using a biogeochemistry
934 model in simulating forests productivity responses to climatic change and [CO_2]
935 increase: example of *Pinus halepensis* in Provence (south-east France), *Ecol.*
936 *Model.*, *166*, 239–255.
937 Raulier, F., P. Y. Bernier, and C. H. Ung (2000), Modeling the influence of temperature
938 on monthly gross primary productivity of sugar maple stands, *Tree Physiol.*, *20*,
939 333–345.
940 Raulier, F., P. Y. Bernier, C.-H. Ung, and R. Boutin (2002), Structural differences and
941 functional similarities between two sugar maple (*Acer saccharum*) stands, *Tree*
942 *Physiol.*, *22*, 1147–1156.
943 Reich, P. B., S. E. Hobbie, T. Lee, D. S. Ellsworth, J. B. West, D. Tilman, J. M. H.
944 Knops, S. Naeem, and J. Trost (2006), Nitrogen limitation constrains sustainability
945 of ecosystem response to CO_2, *Nature*, *440*, 922–925.
946 Ryan, M. G. (1991), A simple method for estimating gross carbon budgets for vegetation
947 in forest ecosystems, *Tree Physiol.*, *9*, 255–266.
948 Schubert, S. D., M. J. Suarez, P. J. Pegion, R. D. Koster, and J. T. Bacmeister (2004), On
949 the cause of the 1930s Dust Bowl, *Science*, *303*, 1855–1859.
950 Sellers, P.J., et al. (1997), BOREAS in 1997: experiment overview, scientific results, and
951 future directions. *J. Geophys. Res.*, *102*, 28731–28769.
952 Ste-Marie, C., D. Paré, and D. Gagnon (2007), The contrasting effects of aspen and jack
953 pine on soil nutritional properties depend on parent material, *Ecosystems*, *10*, 1299–
954 1310.

955 St. George, S., D. M. Meko, M. P. Girardin, G. M. MacDonald, E. Nielsen, G. T.
956 Pederson, D. J. Sauchyn, J. C. Tardif, and E. Watson (2009), The tree-ring record of
957 drought on the Canadian Prairies. *J. Climate*, *22*, 689–710.
958 Su, H., W. Sang, Y. Wang, and K. Ma (2007), Simulating *Picea schrenkiana* forest
959 productivity under climatic changes and atmospheric CO_2 increase in Tianshan
960 Mountains, Xinjiang Autonomous Region, China. *For. Ecol. Manag.*, *246*, 273–
961 284.
962 Tardif, J. (2004), Fire history in the Duck Mountain Provincial Forest, Western Manitoba,
963 Sustainable Forest Management Network. Project Reports 2003/2004 Series, 30 pp.,
964 University of Alberta, Edmonton, Alberta.
965 (www.sfmnetwork.ca/docs/e/PR_200304tardifjfire6fire.pdf)
966 Vincent, L.A., and D. W. Gullett (1999), Canadian historical and homogeneous
967 temperature datasets for climate change analyses, *Int. J. Climatol.*, *19*, 1375–1388.
968 Volney, W.J.A. (1988), Analysis of historic jack pine budworm outbreaks in the Prairie
969 provinces of Canada, *Can. J. For. Res.*, *18*, 1152–1158.
970 von Storch, H., and F. W. Zwiers (1999), *Statistical Analysis in Climate Research*, 484
971 pp., Cambridge University Press, Cambridge, UK.
972 Wang, X. Z. (2007), Effects of species richness and elevated carbon dioxide on biomass
973 accumulation: a synthesis using meta-analysis. *Oecologia*, *152*, 595–605.
974 Wigley, T. M. L., K. R. Briffa, and P. D. Jones (1984), On the average value of correlated
975 time series, with applications in dendroclimatology and hydrometeorology. *J.*
976 *Climate Appl. Meteor.*, *23*, 201–213.

977 Yamaguchi, D. K. (1991), A simple method for cross-dating increment cores from living
978 trees, *Can. J. For. Res.*, *21*, 414–416.
979 Zhou, L., C. J. Tucker, R. K. Kaufmann, D. Slayback, N. V. Shabanov, and R. B. Myneni
980 (2001), Variations in northern vegetation activity inferred from satellite data of
981 vegetation index during 1981–1999, *J. Geophys. Res.*, *106*, 20069–20083.
982

Figures

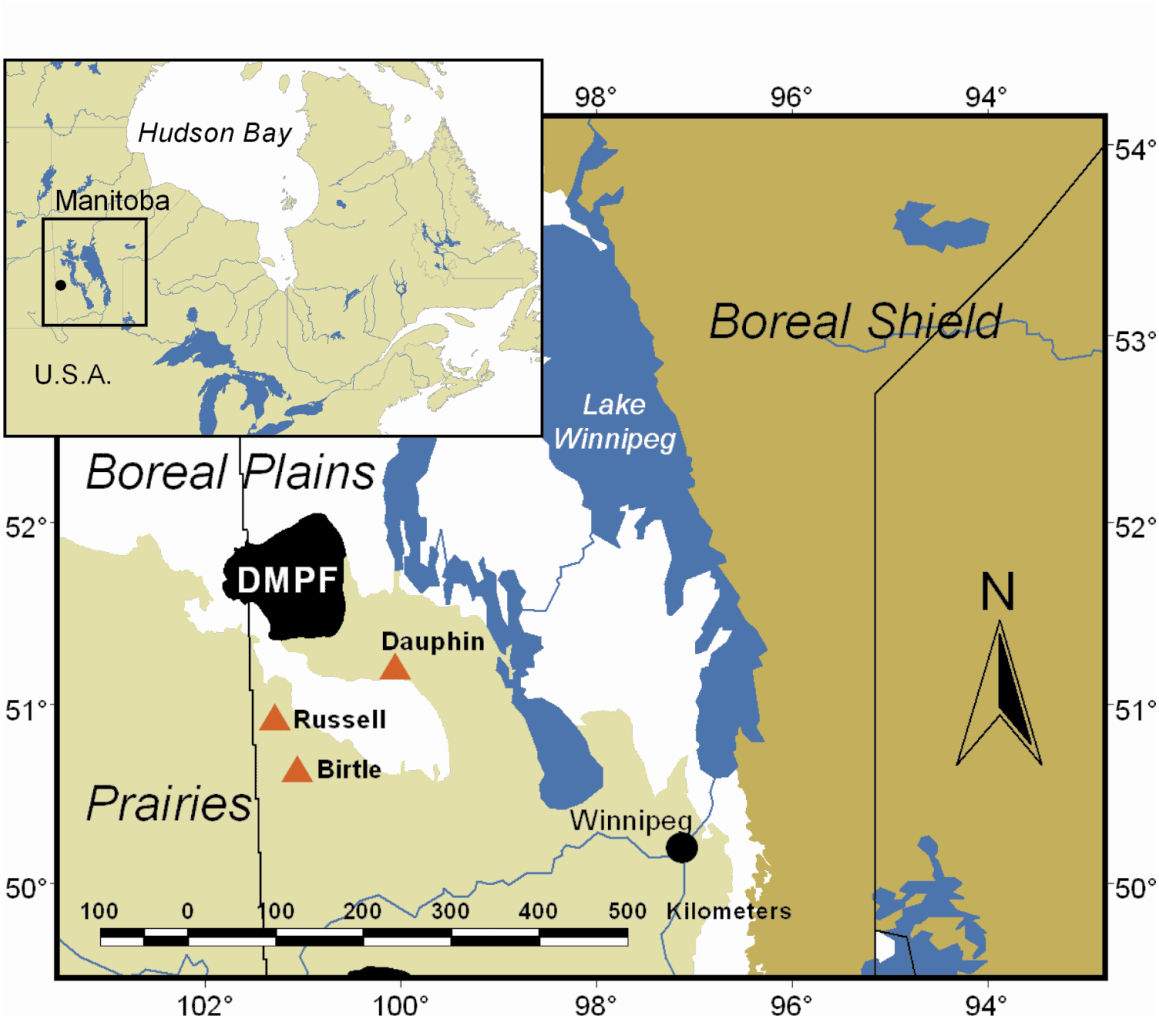

Fig. 1 Map showing the geographical location of Duck Mountain Provincial Forest (DMPF) in Manitoba, Canada. Meteorological stations are indicated by filled triangles.

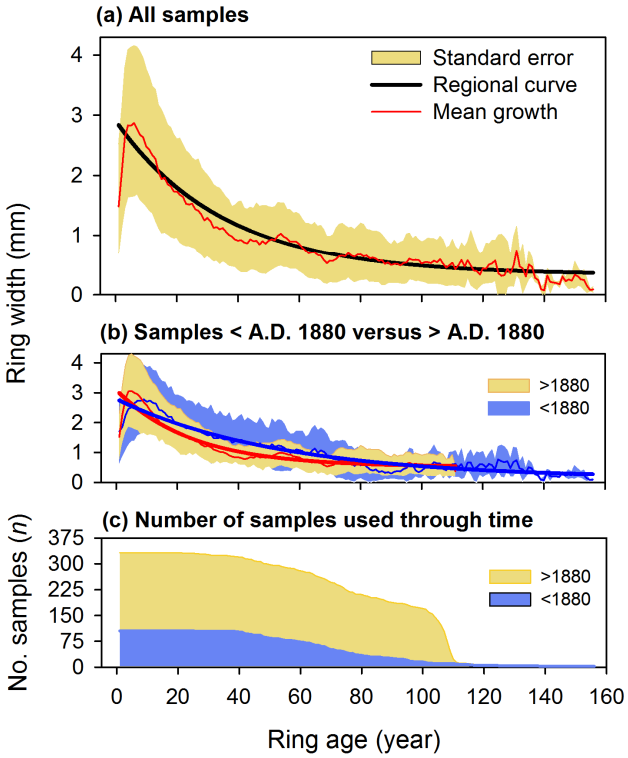

990

991 **Fig. 2** a) The regional curve used in the detrending of the 332 jack pine ring-width
992 measurement series (thick black line). Gray shaded area shows standard error associated
993 with the mean growth of trees (red line) for each ring age. b) Regional and mean growth
994 curves for trees established prior to and after A.D. 1880. c) Total number of samples (*n*)
995 used through time (colors refer to dates of tree establishment). Refer to auxiliary
996 materials Figs. S1 and S2 for sensitivity analyses of these curves.

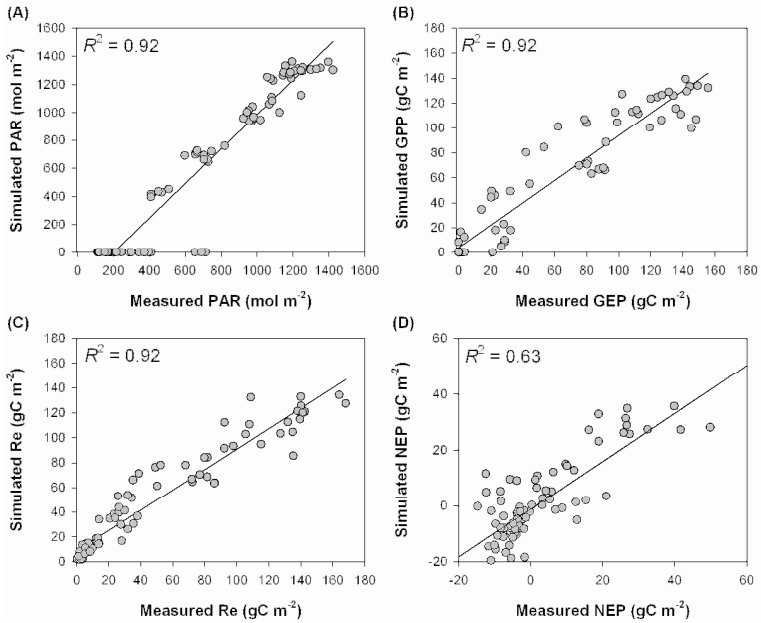

997

998 **Fig. 3** Comparison of monthly simulated fluxes by StandLEAP with those measured by
999 eddy covariance technique over 2000–2006 in a 95-year-old stand in Saskatchewan,
1000 Canada (53.92°N, 104.69°W) [*Gower et al.*, 1997; *Griffis et al.*, 2003]. Data shown are a)
1001 photosynthetically active radiation (PAR), b) gross primary productivity (GPP) versus
1002 gross ecosystem productivity (GEP), c) ecosystem respiration (Re), and d) net ecosystem
1003 productivity (NEP). Linear regression lines with model R-squared are shown. The eddy
1004 covariance technique is a well-established method to directly measure fluxes and net
1005 ecosystem productivity over a fetch larger than typical plot level measurements
1006 (*Baldocchi*, 2003). The methods used for flux measurements follow the methodology
1007 described in *Baldocchi et al.* [2001]. All fluxes were corrected for storage changes in the
1008 canopy atmosphere. Stand attributes for StandLEAP simulation were: stem density =
1009 1190 stems ha^{-1}; aboveground biomass = 69.0 Mg ha^{-1}; depth of available soil water = 1.0
1010 m; elevation 579.27 m [*Gower et al.*, 1997].

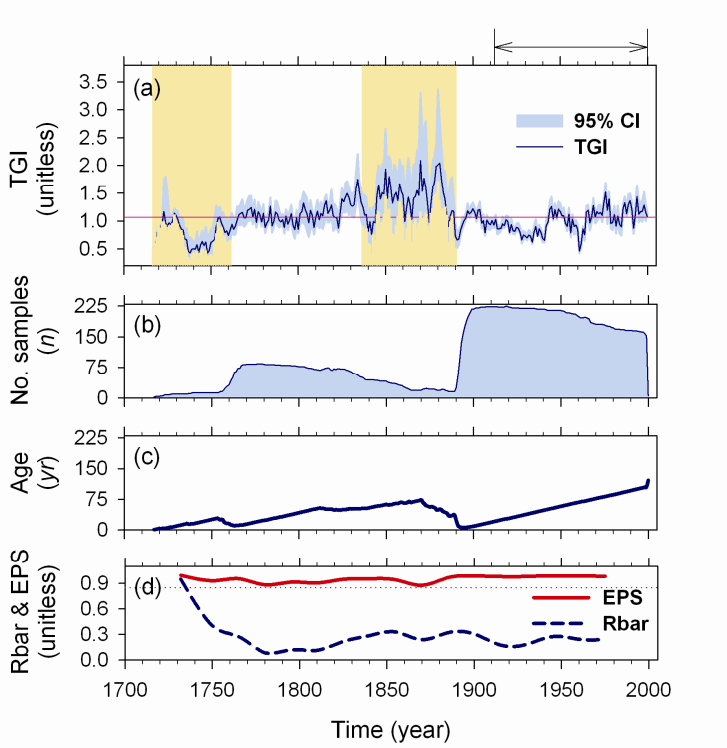

Fig. 4 a) Jack pine tree growth index (TGI) (AD 1717–2000) with 95% bootstrap confidence interval (95% CI; blue shading). A solid line (red) shows the long-term mean; a double arrow (dark grey) delineates the period of analysis 1912–2000 used in the bioclimatic modelling experiment. The vertical shading (yellow) denotes periods with low sample sizes and large error (larger confidence intervals). b) Number of tree rings used through time (divide by 2 for an approximate number of trees). c) Mean cambial age of each calendar year. d) EPS and *Rbar* statistics (calculated over 30 years lagged by 15 years). The dotted line denotes the 0.85 EPS criterion for signal strength acceptance [*Wigley et al.*, 1984].

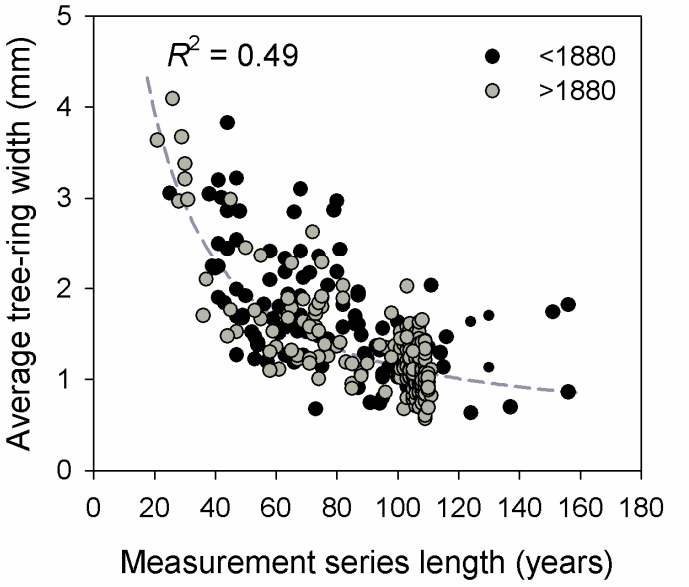

Fig. 5 Relationship between average ring width and length of measurement series for each jack pine series. The diagram differentiates between pre- and post-1880 age cohorts. An exponential fitting is shown along with model fit. The presence of an age-dependent, decreasing relationship between average tree-ring width and measurement series length suggests the existence of a relatively homogeneous behaviour in the growth rates of trees, a necessary condition for application of the regional curve standardization method (*Esper et al.*, 2003).

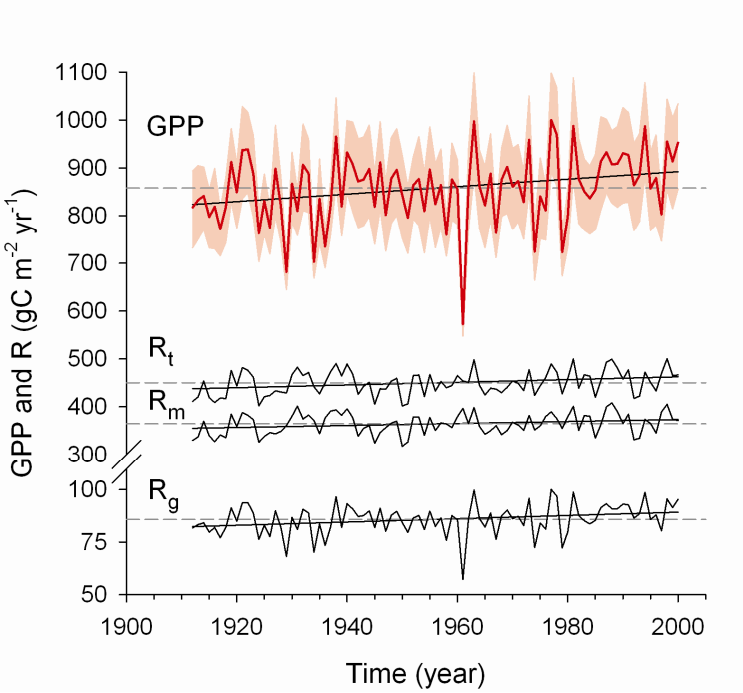

Fig. 6 Simulated annual (January to December) gross primary productivity (GPP) and respiration (growth R_g, maintenance R_m and total R_t) over 1912–2000. Shaded area delineates the 95% confidence interval for uncertainty in the mean GPP. Trend lines applied on data are shown; see Table 2 for model statistics.

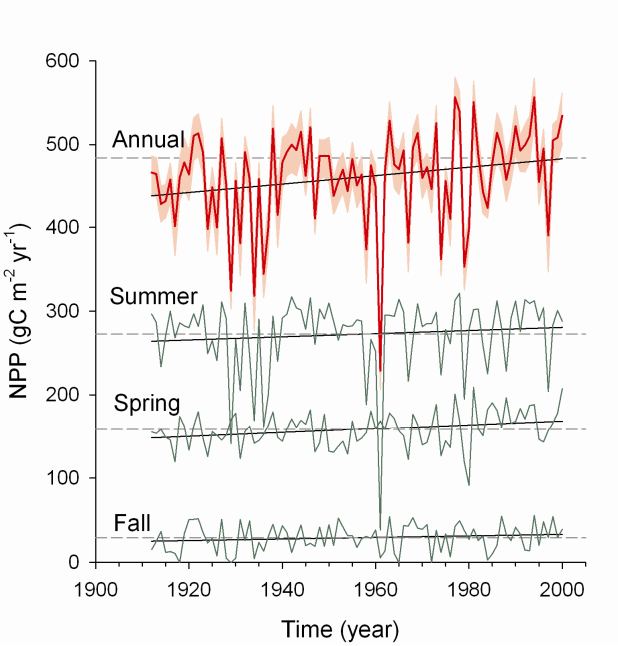

Fig. 7 Simulated net primary productivity (NPP) for spring (March to May), summer (June to August), fall (September to November), and annually (January to December; shaded area delineates the 95% confidence interval for uncertainty in the mean) over 1912–2000. Trend lines applied to data are shown; see Table 2 for model statistics. First-order autocorrelation (AR1) values are 0.02, 0.03, 0.11 and 0.02, respectively.

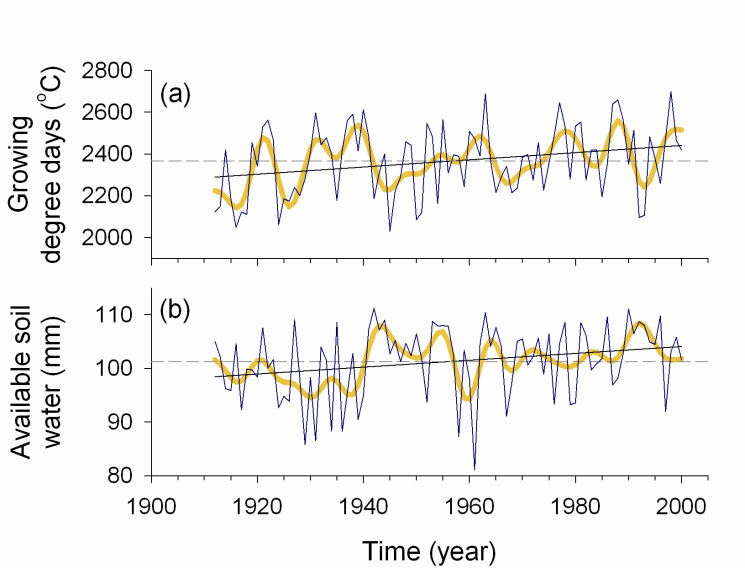

Fig. 8 Trend line applied to a) annual sums of growing degree days above 5°C and b) seasonal average (April-September) of available soil water at depth of 1 m. See Table 2 for model statistics. Thick lines are 5-year polynomial smoothing across data.

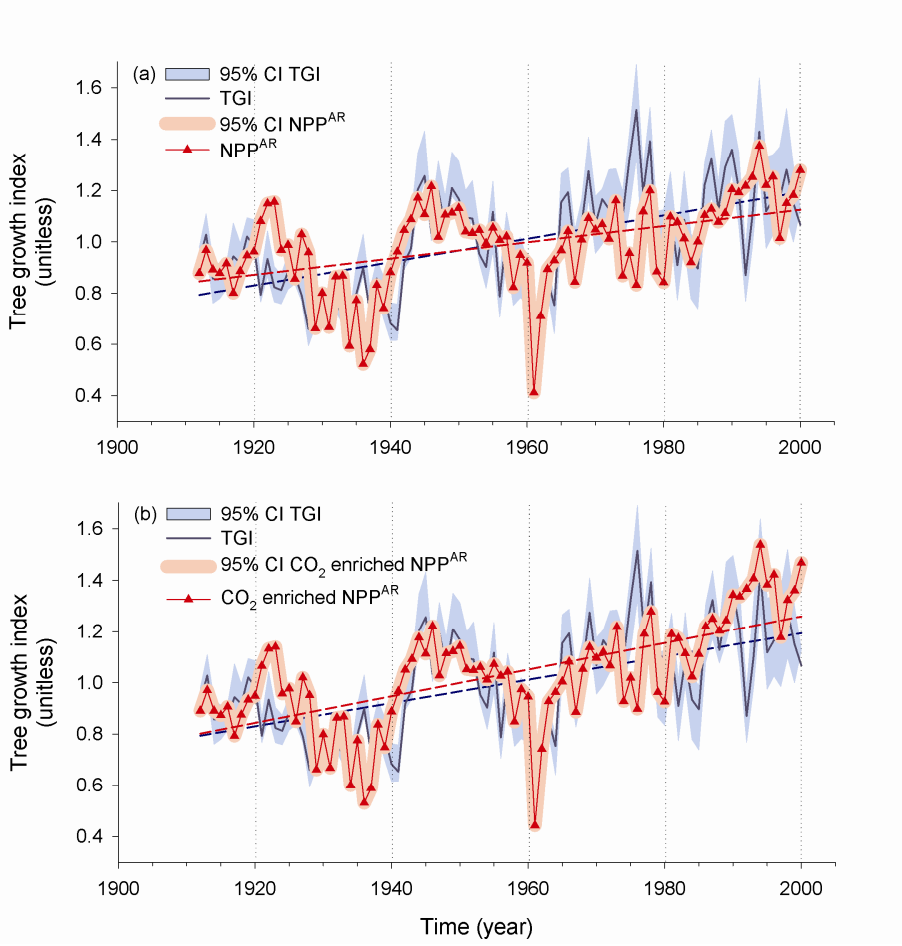

Fig. 9 a) Tree growth index (TGI) versus the AR simulated net primary productivity (NPP^{AR}) over 1912–2000 (both are unitless indices), with linear trend lines across the data (dashed lines; see Table 2 for model statistics). Shaded area: 95% bootstrap confidence interval for uncertainty in the mean TGI and NPP^{AR} (as in Figures 4a and 7). b) Tree growth index (TGI) versus AR simulated net primary productivity (NPP^{AR}) in a CO_2 enriched scenario. The CO_2 enriched simulation is incremented using a logarithmic response function so that NPP achieves an increase of 23% in a doubled CO_2 world (specified parameter $\beta = 0.34$; see text, eq. 9). The CO_2 enriched simulation was achieved using annual averages of atmospheric concentrations of CO_2 reconstructed from ice cores and recorded at Mauna Loa Observatory since 1953.

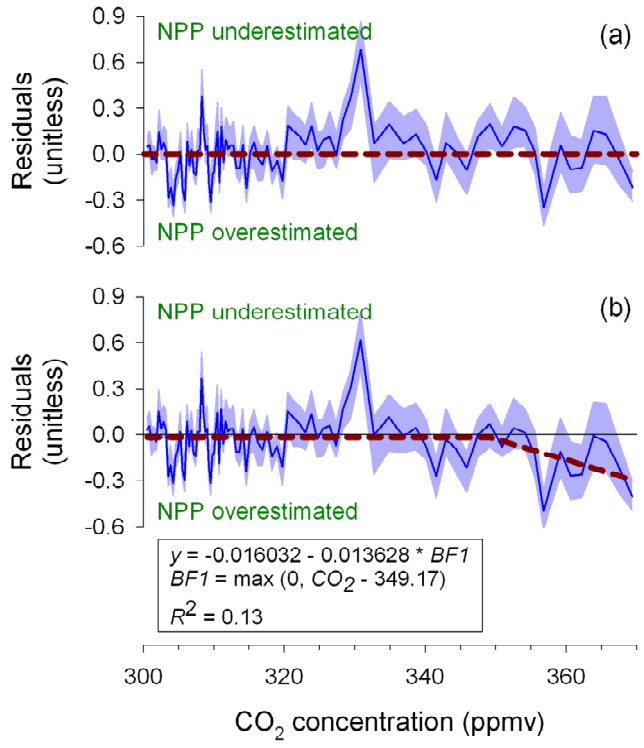

Fig. 10 Residuals of the difference between a) TGI and NPP^{AR} and b) TGI and CO_2 enriched NPP^{AR} (specified parameter $\beta = 0.34$) plotted against annual averages of atmospheric concentrations of CO_2 reconstructed from ice cores and recorded at Mauna Loa Observatory since 1953. Shaded area delineates the 95% confidence interval computed from the square root of the sum of squared errors for TGI and NPP^{AR}. The dashed line shows the relationship between the residuals and atmospheric concentrations of CO_2 modeled using piecewise regression. In (a) the model is suggested to be an intercept-only model; in (b) the relationship takes an inflection point at 349.17 ppmv, suggesting an overestimation of the rate of increase in forest productivity in the last decades of our simulation.

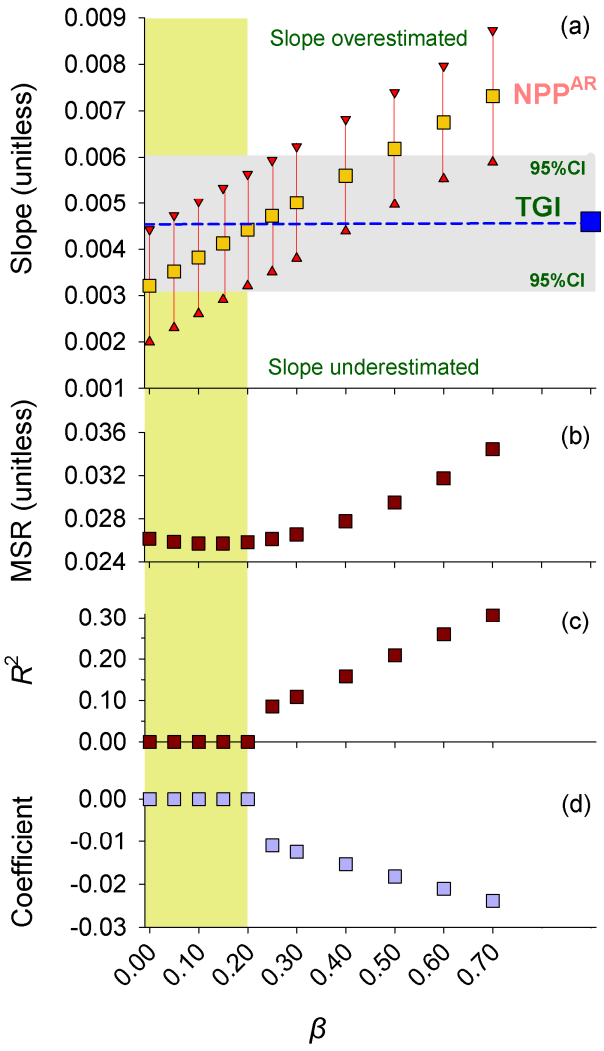

Fig. 11 Sensitivity analysis of the addition of an expected fertilization effect to NPP simulation under a parameter β ranging from 0 to 0.70 (see Methods). a) Slope of the linear trend lines across NPP^{AR} and TGI data (period 1912–2000) with 95% confidence interval (95% CI) (*errors bars* for NPP^{AR} and *horizontal shading* for TGI; adjusted for autocorrelation). b) Mean of squares of the residuals (MSR) of the difference between TGI and NPP^{AR}. c) *R*-squared of the modelled relationship between the residuals of the difference between TGI and NPP^{AR} and atmospheric concentrations of CO_2 as tested using piecewise regression (refer to Fig. 10). d) Coefficients applied to the basis functions that define the slopes of the non-zero sections. Modelled relationships at $\beta > 0.20$ all took

an inflection point at 349.17 ppmv; other models were suggested to be intercept-only models. Results in b), c) and d) suggest an absence of bias in residuals attributed to an over-estimated fertilization effect for values of β ranging from 0 to 0.20 (*vertical shading*).

Tables

Table 1. Summary of the estimated autoregressive (AR) model

Parameter estimates	
Akaike information criterion (AIC) for each AR order	
AR(0)	1402.31
AR(1)	1349.69
AR(2)	1347.60
AR(3)	1348.18
Selected autoregression order	2
Autoregression coefficients	
*p*1	0.495
*p*2	0.184
R^2 due to pooled autoregression	0.39

p: autoregressive (AR) coefficients (see eq. 8 in text)

Period of analysis: 1880–2000

Table 2. Summary of linear trend models on tree growth index (TGI), gross primary productivity (GPP), net primary productivity (NPP and NPP after application of the AR model, Table 2), respiration (growth R_g, maintenance R_m and total R_t), growing degree days above 5°C (GDD), vapour pressure deficit (VPD), and soil water content at a depth of 1 m (SWC) over the period 1912–2000.

Variable	R^2	**Slope**	**Effective *n***	***t*-value**	**Probability**
Annual GPP [A]	0.097	+0.780 (gC m^{-2} yr^{-1})	102	3.285	***
Annual R_m [A]	0.051	+0.078 (gC m^{-2} yr^{-1})	64	1.835	*
Annual R_g [A]	0.097	+0.204 (gC m^{-2} yr^{-1})	102	3.285	***
Annual R_t [A]	0.078	+0.282 (gC m^{-2} yr^{-1})	71	2.421	**
Annual NPP [A]	0.078	+0.502 (gC m^{-2} yr^{-1})	98	2.838	**
Spring NPP (March-May) [A]	0.083	+0.233 (gC m^{-2} yr^{-1})	90	2.830	**
Summer NPP (June-August) [A]	0.021	+0.188 (gC m^{-2} yr^{-1})	98	1.442	N.S.
Fall NPP (September-November) [A]	0.023	+0.092 (gC m^{-2} yr^{-1})	102	1.533	N.S.
Annual NPP^{AR}	0.258	+0.0032 (unitless) 95% CI [0.0020, 0.0044]	N.A.	N.A.	**
Annual CO_2-enriched NPP^{AR} (β = 0.34)	0.386	+0.0044 (unitless) 95% CI [0.0032, 0.0056]	N.A.	N.A.	***
Annual TGI [B]	0.344	+0.0046 (unitless) 95% CI [0.0032, 0.0060]	N.A.	N.A.	**
Residuals (TGI – NPP^{AR})	0.045	+0.001 (unitless)	N.A.	N.A.	N.S.

Annual sums of GDD	0.060	+0.073 (°C)	68	2.055	**
Annual average of VPD	0.000	-0.023 (Pascal)	61	0.082	N.S.
Seasonal average (April-September) of SWC	0.068	+0.064 (mm)	93	2.058	**

*** Significant at $P \leq 0.01$

** Significant at $P \leq 0.05$

* Significant at $P \leq 0.10$

N.S.: Not significant

N.A.: Not available

[A] Significance of the linear trend was examined using least-squares linear regressions [*von Storch and Zwiers*, 1999]. Goodness of fit is described by the coefficient of determination (R^2). Significance was tested against the null hypothesis that the trend is different from zero, using a variant of the t test with an estimate of the effective sample size (effective *n*) that takes into account the presence of serial persistence in data.

[B] Significance of trends was evaluated using Monte Carlo simulations (see Methods).